Fracture Mechanics of Concrete Structures, de Borst et al (eds) © 2001 Swets & Zeitlinger, Lisse, ISBN 90 2651 825 0

Cohesive multiscale 3-D FE model applied to study the dynamyc mixed-mode fracture of concrete

G.Ruiz
ETSI Caminos, C. y P, Universidad de Castilla-La Mancha, 13071 Ciudad Real, Spain
A.Pandolfi
Dipartimento di Ingegneria Strutturale, Politecnico di Milano, 20133 Milano, Italy
M.Ortiz
Graduate Aeronautical Laboratories, California Institute of Technology, Pasadena, CA 91125, USA

ABSTRACT: A cohesive formulation of fracture is taken as a basis for the simulation of processes of combined tension-shear damage and mixed-mode fracture in specimens subjected to dynamic loading. We account explicitly for microcracking, the development of macroscopic cracks and inertia, and the effective dynamic behavior of the material is predicted as an outcome of the calculations. In particular, a shear-tension damage coupling arises as a direct consequence of slanted microcrack formation in the process zone. The particular configuration contemplated in this study is the three point bend beam with a precrack shifted from the central cross section, leading to asymmetrical loading conditions and the development of a mixed-mode process zone. The model is able to capture closely the experimentally observed fracture patterns and crack extension histories, as a function of pre-crack geometry and loading conditions. In particular, it correctly accounts for the competition beetween crack-growth and nucleation mechanisms.

1 INTRODUCTION

In this paper we use cohesive theories of fracture to simulate processes of tension-shear damage and mixed-mode fracture in concrete specimens subjected to dynamic loading. We adopt a simple cohesive law proposed by Camacho and Ortiz (Camacho & Ortiz 1996) which accounts for tension-shear coupling through the introduction of an effective scalar opening displacement. The form of the effective opening displacement allows for different weights to be applied to the normal and tangential components of the opening displacement vector. This simple device also permits according the material critical normal and shear tractions bearing arbitrary ratios. This flexibility is particularly important in the case of concrete, where the aggregate interlocking mechanism may result in critical shear tractions greatly in excess of the tensional strength of the material. The cohesive behavior of the material is assumed to be rigid, or perfectly coherent, up to the attainment of an effective traction, at which point the cohesive surface begins to open. The cohesive law is rendered irreversible by the assumption of linear unloading to the origin.

In calculations, we allow for decohesion to occur along element boundaries only. Initially, all element boundaries are perfectly coherent and the elements are conforming in the usual sense of the displacement finite element method. When the critical cohesive traction is attained at the interface between two volume elements, we proceed to insert a cohesive element at that location. Crack nucleation is thus accounted for and falls within the scope of the analysis. The cohesive element subsequently governs the opening of the cohesive surface. It is important to note that the cohesive size of concrete scales with the aggregate size. Since, as noted earlier, this cohesive length must be resolved numerically, the element size must be of the order of the aggregate size over the cohesive zone. Thus, the insertion of a new cohesive element may be regarded as the nucleation of one additional microcrack. These microcracks may subsequently coalesce among themselves, resulting in the nucleation and growth a structural crack.

Since the fracture surface is confined to inter-element boundaries, the structural cracks predicted by the analysis are necessarily *rough*. Cracks in concrete, as well as in materials which crack by intergranular fracture, exhibit considerable roughness on the scale of the aggregate or grain size. The surface roughness adds to the fracture area and, consequently, increases the specific fracture energy. Severe roughness may also toughen the material by the aggregate interlocking and crack bridging mechanisms. By the choice of an element size comparable to the aggregate size, the numerical model furnishes a simple description of the actual crack-surface roughness which is observed experimentally and the attendant effective toughening of the material.

It is also important to note that, owing to the presence of profuse microcracking in the vicinity of the crack tip, the *effective* fracture behavior of the

material may differ significantly from that which obtained by exercising the cohesive law directly. In particular, when a pre-crack is subjected to pure mode II loading a number of slanted microcracks are inevitably formed ahead of the crack tip, roughly at 45° to the plane of the pre-crack. The subsequent behavior of the crack is then sensitively dependent on the extent of normal compression, which tends to close the trailing microcracks and constrains them to undergo frictional sliding. Evidently, this type of behavior is not hardwired into the class of cohesive laws adopted here, but it is *predicted* by them.

In addition, the effective dynamic behavior of the material is also predicted as an outcome of the simulations. Indeed, the cohesive properties of the material are assumed to be rate-independent. Cohesive theories, in addition to building a characteristic length into the material description, endow the material with an intrinsic *time scale* as well (Camacho & Ortiz, 1996). This intrinsic time scale permits the material to discriminate between slow and fast loading rates and ultimately allows for the accurate prediction of the dynamic fracture properties (Ruiz et al. 2000).

The particular configuration contemplated in this study is the three point bend beam with a precrack displaced from the central cross section, so that symmetry is broken and a mixed-mode process zone results. The specimens are tested dynamically by means of a Charpy tester (John 1988, John & Shah 1990) or a drop weight device (Guo et al. 1995). This type of test furnishes a demanding validation of the theory, since in as much as the notch offset is longer, so much the more the shear damage comes into play in the formation and development of the main crack starting from the notch. In addition, enlarging the offset increases the possibility of the formation of alternative crack paths around the central cross section. Indeed, the simulations capture closely fracture patterns, even those in which microcracked zones at different areas of the beam develop simultaneously competing to generate a main crack. They also give accurate histories of the crack extension, and the computed loads also fit the reported experimental load histories.

The organization of the paper is as follows. Next section gives a brief outline of the characteristics of the simulation, and then we present the results regarding the evolution of the fracture zone and compare them with experimental data. Namely this includes the study of the crack patterns, the analysis of the crack initiation and growth, and the examination of the crack extension history. Finally, in the last section we point out some concluding remarks.

2 SIMULATION OF THE INITIATION AND GROWTH OF MIXED-MODE CRACKS IN CONCRETE UNDER DYNAMIC LOADING

We proceed to model the fracture of concrete under mixed-mode loading in the dynamic regime. Specifically we aim at simulating the mixed-mode tests performed by Guo, Kobayashi and Hawkins (Guo et al. 1995) and John and Shah (John 1988, John & Shah 1990). The particular cohesive model employed in calculations and its finite-element implementation can is thoroughly described in Ortiz & Pandolfi (1999). It accounts for the coupling existing between fracture modes by balancing mode I and mode II openings through the ratio between the critical shear and the tensile strength, which we have estimated by analyzing mixed-mode tests (van Mier et al. 1991, Nooru-Mohamed 1992). The details of the fragmentation procedures implemented in the code are explained in Pandolfi & Ortiz (1998). The geometry and dimensions of the prismatic beams used in both experimental programs can be seen in Figure 1. Please observe that in the beams tested by John and Shah the notch offset was not constant, in order to study how the crack initiation and growth is affected by the notch shift. The material parameters in the constitutive equations are taken from the aforementioned papers describing the experimental work. In addition, the load and boundary conditions of the tests are carefully met by the simulations.

Figure 2 shows one of the meshes used in the numerical tests. We use the advancing front method (Radovitzky 1998) to mesh all the surfaces and the interior of the specimens with 10-node quadratic tetrahedra. In order to avoid mesh-sensitiveness, the element size commensurates with half the maximum aggregate size in the areas where the cracking process is expected to take place (Camacho & Ortiz, 1996). Nevertheless, the crack is not given any predetermined starting point or crack path through the initial mesh. On the contrary, it is incumbent to the fragmentation algorithm to determine whether the opening condition, i. e. the attainment of the critical strength by the effective tension, is met or not at the tetrahedral interfaces. In case it is, the model allows the opening of the crack and covers the new surface with cohesive elements.

2.1 *Crack pattern*

It is clear that the most interesting feature of the model is its ability to keep track of the process of fragmentation and fracture, and consequently its competence in predicting complex crack patterns

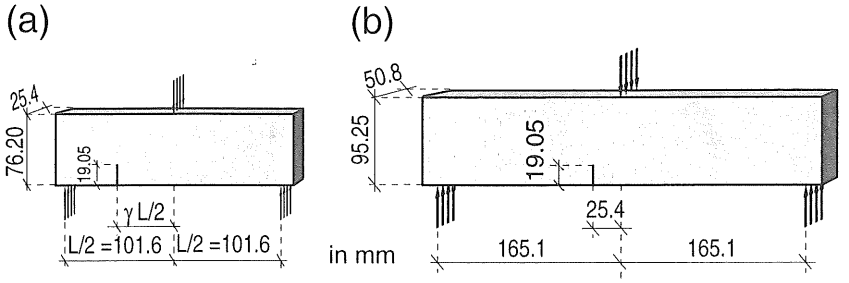

Figure 1. Geometry and dimensions of the beams tested by (a) John and Shah (John 1988, John & Shah 1990) and (b) Guo, Kobayashi and Hawkins (Guo et al. 1995).

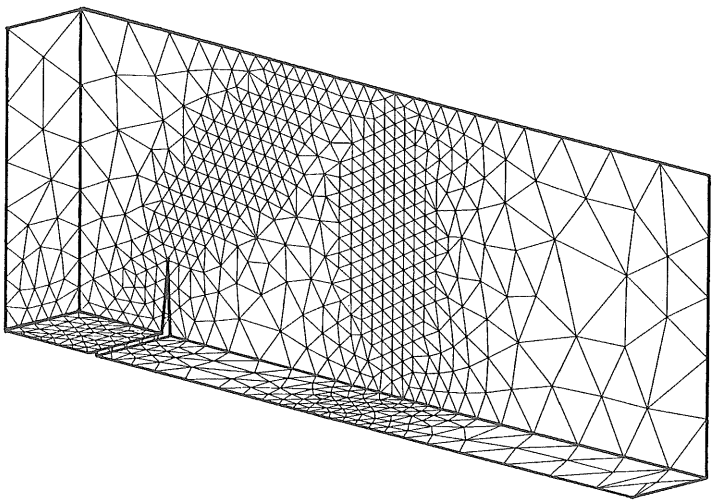

Figure 2. Upward view of one of the meshes generated to simulate the tests by John and Shah.

becomes an important keypoint in its validation (e.g. see Belytschko et al. 1996).

Figure 3 compares the crack pattern obtained in experiments (thick solid lines) with the simulated damage distribution (shade in gray levels meaning the magnitude of the consumption of cohesive energy). The predictions given by the simulations not only are in very good agreement with the actual crack paths, but also give information on the extent of microcracking developed around the main crack and even in other very loaded areas. This is especially noticeable in Figure 3a, since the calculations show a damaged zone at the bottom of the beam, below the load point, far from the main crack propagated from the notch. Actually, there is another crack zone developing in this zone, which finally arrests due to the unloading subsequent to the propagation of the main crack. The existence of this damaged zone far from the main crack discloses sources of energy consumption different from the main crack itself, and thus gives an explanation to scale and dynamic effects on the fracture process, since the distribution of the damage throughout the specimen depends on its geometry and scale relative to the characteristic length and on the loading rate (Ruiz et al. 2000).

2.2 *Crack initiation and growth*

Figure 4 shows four snapshots of a numeric Charpy test reproducing one of the experiments by John and Shah. They are taken at 0.6, 1.0, 1.4 and 1.8 ms from the beginning of the numerical test. The visualization renders only the edges of the cracks, so as to distinguish them from the boundaries of the elements that are not affected by the fracture process. At each shot the specimen is depicted upwards and downwards in order to observe how cracks grow in all the faces of the specimen. As mentioned above, the gray shade represents the extent of damage present in the cracked zone, and it roughly indicates the location of the main crack.

The images for 0.6 ms in Figure 4 show the initiation of the crack at the tip of the notch. The fracture zone rapidly orientates towards the load point, following —in the mean— the same path given by

(a)

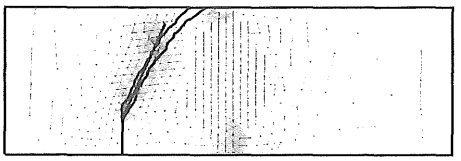

(b)

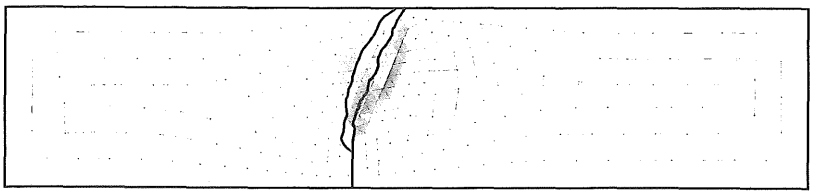

Figure 3. Damage obtained in the simulations compared to the experimental crack pattern —thick solid lines— by (a) John & Shah (1990), and (b) Guo et al. (1995).

the maximum hoop stress criterion (which leads to accurate predictions of crack paths in concrete, see e. g. Gálvez et al. 1998).

The development of the crack zone from the notch does not imply an immediate decrease of the external load, since the stresses transmitted through the lips of the cracks in the first stages of the cracking process are high. Thus, the external load and the intensity of the stresses outside the crack zone continue increasing, and eventually the opening condition is reached at another heavy loaded area, that located at the bottom of the beam below the load point. In fact, the following snapshot, 1.0 ms after the start of the test, shows how several cracks begin to develop at this zone, creating another fracture zone that competes with the one at the notch in the process of generating a main crack by microcracks coalescence. Please, observe that these cracks appear at the bottom of the beam, grow in the shape of a lens and finally get the lateral faces.

The competition between the two fracture zones is won by the one at the notch, as it is shown in the remaining two views of the specimen. In fact, as the damage at the notch increases the stress level is released and finally causes the coalescence process at the bottom of the beam to arrest. In the end it appears another crack zone generated by the strong compression existing right below the load point.

John and Shah pointed out the presence of both fracture zones and the competition between them to generate a main crack (John 1988, John & Shah 1990), since as they moved the notch towards the support they found a transition between the two possible crack patterns. In keeping with their experiments, our calculations automatically predict that the succeeding crack will start from the bottom of the beam after the notch offset surpasses a critical threshold. The simplicity with which the model reproduces such complex transition is another sign of its fidelity to the actual material behavior.

2.3 *Crack extension*

Guo, Kobayashi and Hawkins (Guo et al. 1995) measured the main crack extension history by using standard extensometry combined with moiré interferometry; e. g. see Epstein (1990) for a complete description of this optical technique. Both experimental procedures gave very much the same results, as can be seen in Figure 5. The figure also depicts the crack length history stemming from our calculations, which fits very well the experimental data.

The crack does not grow right after the impact of the tup, for the stress wave needs almost 320 μs to reach the notch and load its tip to the tensile strength. Then a sharp growth of the crack length follows until it stabilizes at the rate of 170 m/s approximately during 200 μs. Finally, the crack slows down as it approaches the boundary of the specimen and there appears some stress relief due to the developing of the fracture process and to the rebounds of the waves at the specimen surfaces. The computed crack length history has an inflexion associated with a period of extension of the microcracked zone in several directions at the same time, that is with an increase of the width of the cracked zone.

The goodness of fit between the real and the simulated histories is especially noticeable if it is considered that the cohesive properties of the material are rate independent in the simulations. The dynamic behavior of concrete comes out from them as a result of the rate sensitiveness emerging from cohesive theories, and of the direct simulation of the microinertia attendant to microcracking and fracture (Camacho & Ortiz 1996, Ruiz et al. 2000).

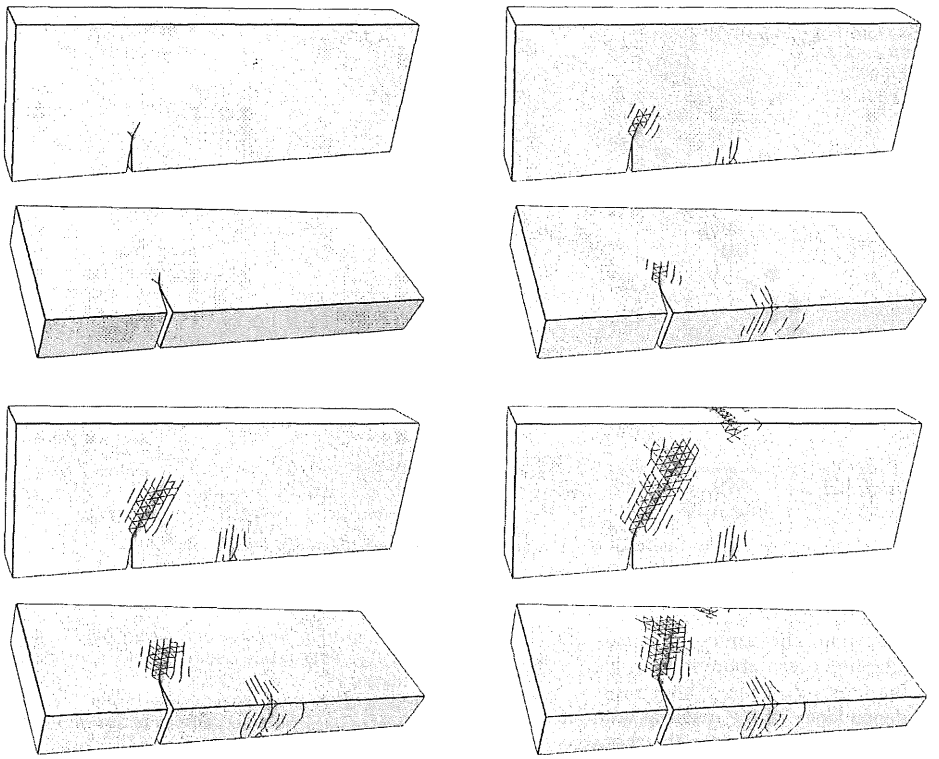

Figure 4. Sequence of snapshots in a Charpy test. Each snapshot is represented by a downward and an upward view, to clearly see the damage at the bottom of the beam. The sequence of images correspond to 0.6, 1.0, 1.4 and 1.8 milliseconds.

3 CONCLUDING REMARKS

We have investigated the feasibility of using cohesive theories of fracture, in conjunction with the direct simulation of fracture and fragmentation, in order to describe processes of tensile and shear damage in concrete specimens subjected to dynamic loading. The particular configuration contemplated in this study is the three point bend beam with a notch shifted from the central cross section, tested dynamically by means of a drop weight device (Guo et al. 1995), or of a modified Charpy tester(John 1988, John & Shah 1990). We reproduced the actual crack pattern found in experiments and other related results as the crack growth extension history.

Our approach resolves explicitly some micromechanical scales, following the multiscale modeling trend to study damage in brittle materials initiated by Camacho and Ortiz (Camacho & Ortiz, 1996). The coupling existing between fracture modes is partly accounted for by an effective constitutive description. It balances mode I and mode II openings by means of the ratio between the critical shear and the tensile strength. We estimated its value by analyzing some very detailed mixed-mode tests (van Mier et al. 1991, Nooru-Mohamed 1992) in a consistent way with our cohesive model assumptions. On the other hand, the mode coupling also comes up as a result of the development of a microcracked zone, because the different slopes of the crack planes result in normal and tangent stress components even in case coupling is not taken into account in the cohesive law. All things considered, most of the phenomena leading to nucleation, orientation and growth of cracks are left to be resolved by the model at the structural level, while few of them are put within the cohesive law.

The ability of the model to predict complex crack patterns becomes an important key point in its validation. It should be noted that many of the cohesive theories implemented so far in finite element codes rely on the knowledge of the crack path in advance, obtained by LEFM simulations or by experimentation. By way of contrast, our simulations are given no hint whatsoever on what the crack path may be and, nevertheless, they capture closely the fracture pattern for different experimental configurations, even those in which there is a competition between microcracked zones at different areas of the beams resulting in a single main crack that does not develop from the notch tip.

The simulations also come up with accurate histo-

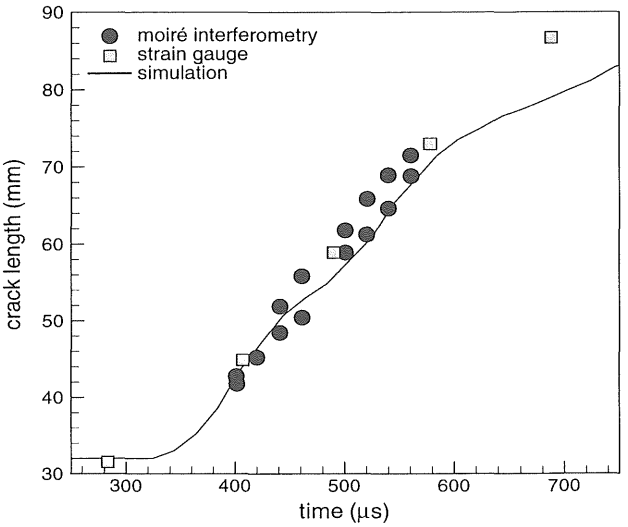

Figure 5. Crack length history in the tests by Guo et al (Guo et al. 1995), which was measured at the same time by strain gauges and moir interferometry. The solid line represents our numerical results.

ries of the crack extension. This can be explained, on the one hand, by the direct resolution of microinertia on the scale of the cohesive zone, which captures most of the rate-dependency of the material without the need of accounting for this effect in the cohesive law. On the other hand, cohesive theories discriminate between slow and fast rates of loading in the same way they do between small and big specimen sizes. By accounting for both effects, the model accurately predicts the dynamic behavior of concrete.

4 ACKNOWLEDGEMENTS

Gonzalo Ruiz gratefully acknowledges financial support from the *Ministerio de Ciencia y Tecnología*, Spain, through grant MAT2000-0705.

5 REFERENCES

Belytschko, T., Krongauz, Y., Organ, D., Fleming, M. and Krysl P. 1996. Meshless methods: an overview and recent developments. *Computer Methods in Applied Mechanics and Engineering* 139:3-47.

Camacho, G. T. and Ortiz M. 1996. Computational modelling of impact damage in brittle materials. *International Journal of Solids and Structures* 33(20-22):2899-2938.

Epstein, J. S. (Ed.) 1990. Special issue on moiré interferometry. *Optics and Lasers in Engineering* 12(2-3).

Gálvez, J. C., Elices, M., Guinea, G. V. and Planas, J. 1998. Mixed mode fracture of concrete under proportional and nonproportional loading. *International Journal of Fracture* 94:267-284.

Guo, Z. K., Kobayashi, A. S. and Hawkins, N. M. 1995. Dynamic mixed mode fracture of concrete. *International Journal of Solids and Structures* 32(17/78):2591-2607.

John, R. 1988. *Mixed-Mode Fracture of Concrete Subjected to Impact Loading*. PhD thesis, Northwestern University, Evanston, Illinois.

John, R. and Shah, S. P. 1990. Mixed-mode fracture of concrete subjected to impact loading. *Journal of Structural Engineering* 116(3):585-602.

Nooru-Mohamed, M. B. 1992. *Mixed-Mode Fracture of Concrete: an Experimental Approach*. PhD thesis, Delft University of Technology, Netherlands.

Ortiz, M. and Pandolfi, A. 1999. Finite-deformation irreversible cohesive elements for three-dimensional crack-propagation analysis. *International Journal for Numerical Methods in Engineering* 44(9):1267-1282.

Pandolfi, A. and Ortiz, M. 1998. Solid modeling aspects of three-dimensional fragmentation. *Engineering with Computers* 14(4):287-308.

Radovitzky, R. 1998. *Error estimation and adaptive meshing in strongly nonlinear dynamic problems*. PhD thesis, California Institute of Technology, Pasadena, California.

Ruiz, G., Pandolfi, A. and Ortiz, M. 2000. Finite-element simulation of the dynamic Brazilian tests on concrete cylinders. *International Journal for Numerical Methods in Engineering* 48:963-994.

van Mier, J. G. M., Nooru-Mohamed, M. B. and Timmers, G. 1991. An experimental study of shear fracture and aggregate interlock in cement based composites. *Heron* 36(4).